Investigations on η’ photoproduction off near-free neutron at Graal

31st International Workshop on Deep Inelastic Scattering

Antonio Riggio
University of Messina MIFT, INFN sec. Catania
Antonio.Riggio@studenti.unime.it

Outlook

- **Motivations of research**
- **Description of the apparatus**
- **Analysis and results**
- **Conclusions**

Motivations of the research

1 To study the excitation spectrum of the nucleons by excitating them with electromagnetic sounds like photons or electrons.

2 Comparing excited states of the nucleons with the ones predicted by models about the inner structure of the nucleon.

Elastic and inelastic scattering reactions π p were intensively used in the past

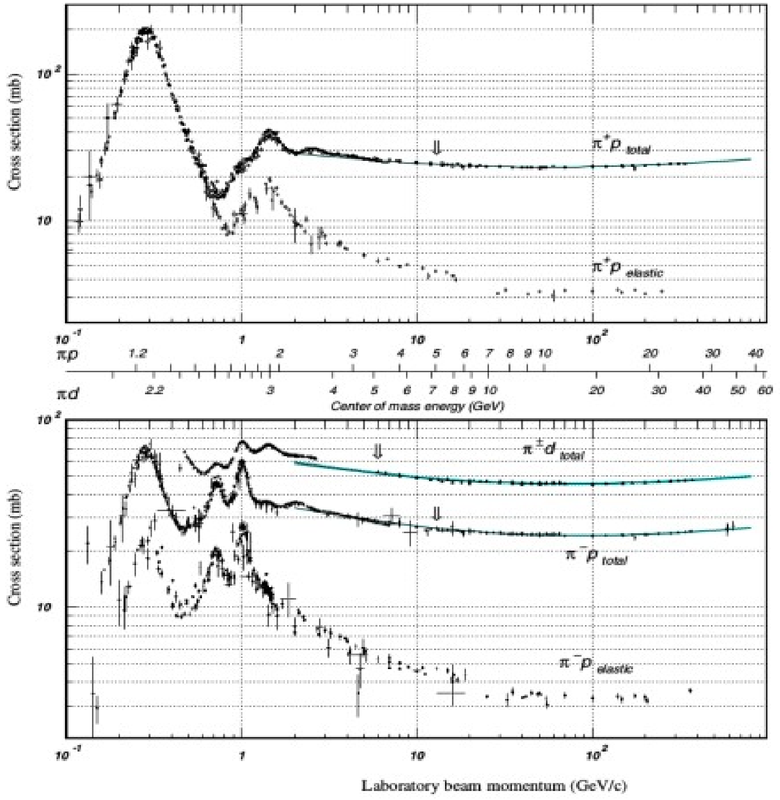

http://pdg.lbl.gov/current/xsect/,
courtesy of the COMPAS group, IHEP, Protvino.

Advantages

1 High cross sections values.

2) Possibility to explore the isospin degrees of freedom of resonances.

Drawbacks

“Missing” resonances

Meson photoproduction reactions

Advantages

1 scanning a wider range of resonances.

2 access to polarizzation observables by using polarized beam and target.

Drawbacks

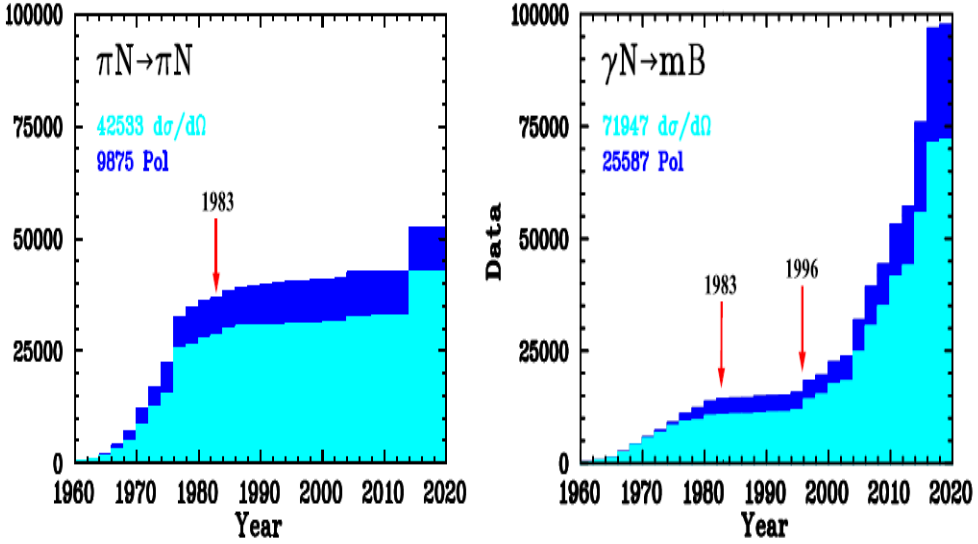

How to excite barionic resonances

- Pions-nucleon scattering reactions (they allow discovery of the Δ resonance).
- Meson photoproduction reactions

Motivations of research

Pseudoscalar Meson photoproduction reactions on nucleons

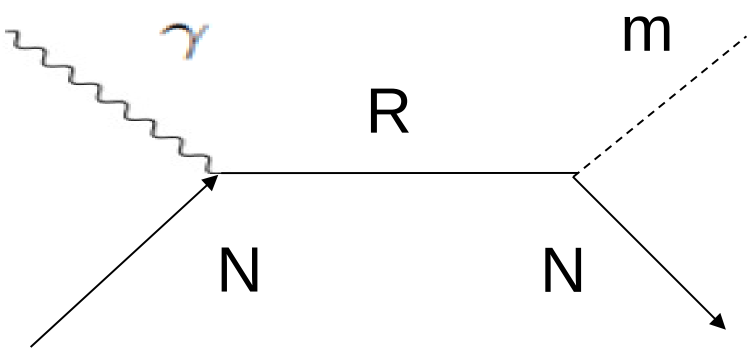

- Excited states of nucleons as intermediated states(resonances) in these process.
- Decay by strong interaction with the emisison of mesons.

η and η' photoproduction channels

- Isospin filters (only N* resonances can contribute).

Notation used for resonances

$$L_{2I2J}$$

L angular momentum of the sistem meson-nucleon in the C.M.

Experimental excitation spectrum of nucleons

N*	Status	SU(6) ⊗ O(3)	Parity	Δ*	Status	SU(6) ⊗ O(3)
P11(938)	****	$(56,0^+)$	+	P33(1232)	****	$(56,0^+)$
S11(1535)	****	$(70,1^-)$				
S11(1650)	****	$(70,1^-)$		S31(1620)	****	$(70,1^-)$
D13(1520)	****	$(70,1^-)$	−	D33(1700)	****	$(70,1^-)$
D13(1700)	***	$(70,1^-)$				
D15(1675)	****	$(70,1^-)$				
P11(1520)	****	$(56,0^+)$		P31(1875)	****	$(56,2^+)$
P11(1710)	***	$(70,0^+)$		P31(1835)		$(70,0^+)$
P11(1880)		$(70,2^+)$				
P11(1975)		$(20,1^+)$				
P13(1720)	****	$(56,2^+)$		P33(1600)	***	$(56,0^+)$
P13(1870)	*	$(70,0^+)$		P33(1920)	***	$(56,2^+)$
P13(1910)		$(70,2^+)$	+	P33(1985)		$(70,2^+)$
P13(1950)		$(70,2^+)$				
P13(2030)		$(20,1^+)$				
F15(1680)	****	$(56,2^+)$		F35(1905)	****	$(56,2^+)$
F15(2000)	**	$(70,2^+)$		F35(2000)	**	$(70,2^+)$
F15(1995)		$(70,2^+)$				
F17(1990)	**	$(70,2^+)$		F37(1950)	****	$(56,2^+)$

Motivations of the research

Two tecniques used for the production of the γ-ray beam

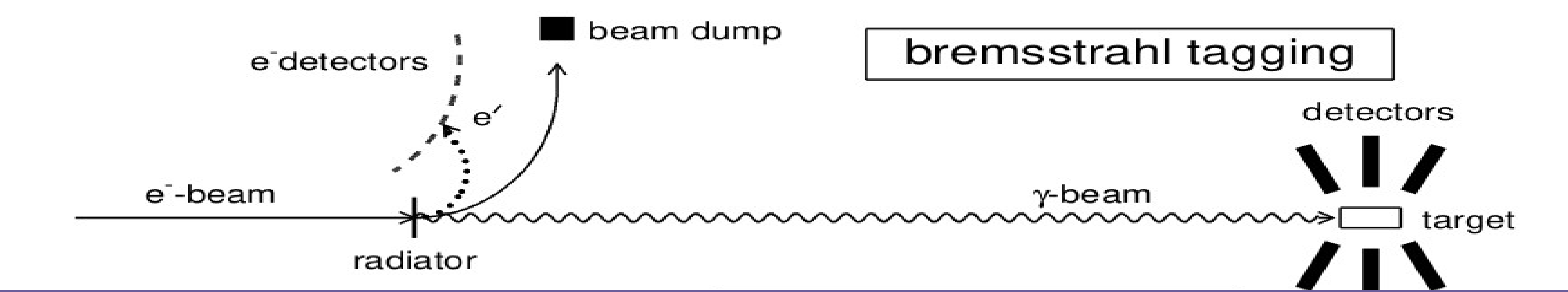

ELSA, JLAB(CLAS), MAMI

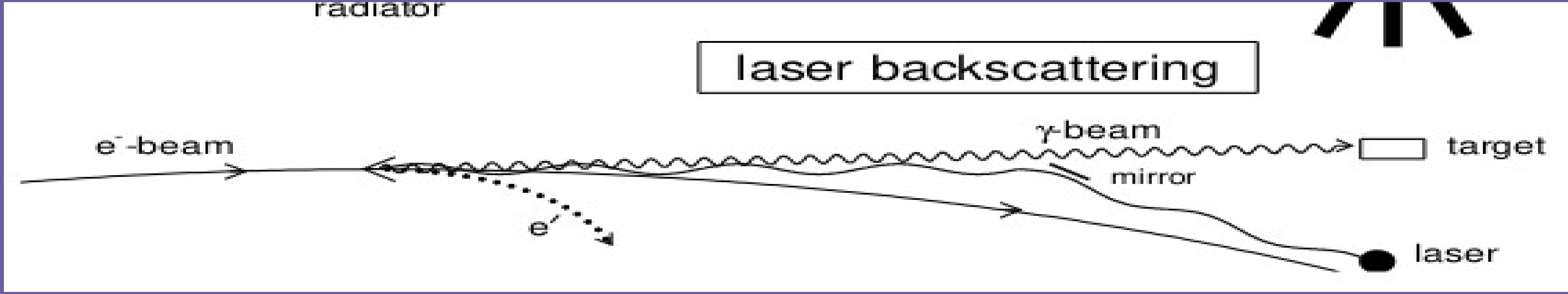

BNL(LEGS) , ESRF(GRAAL), SPring8(LEPS)

Motivations of the research

Resonances decay by strong interaction with mean-life tau ~ 10^(-26) s.

Their peaks are associated to Width~ 100 MeV and distances ~ 10 MeV

Sovrappositions occur in the toral cross section spectra

Total photoabsorption cross section on proton and neutron

http://arxiv.org/abs/nucl-ex/0306023v1

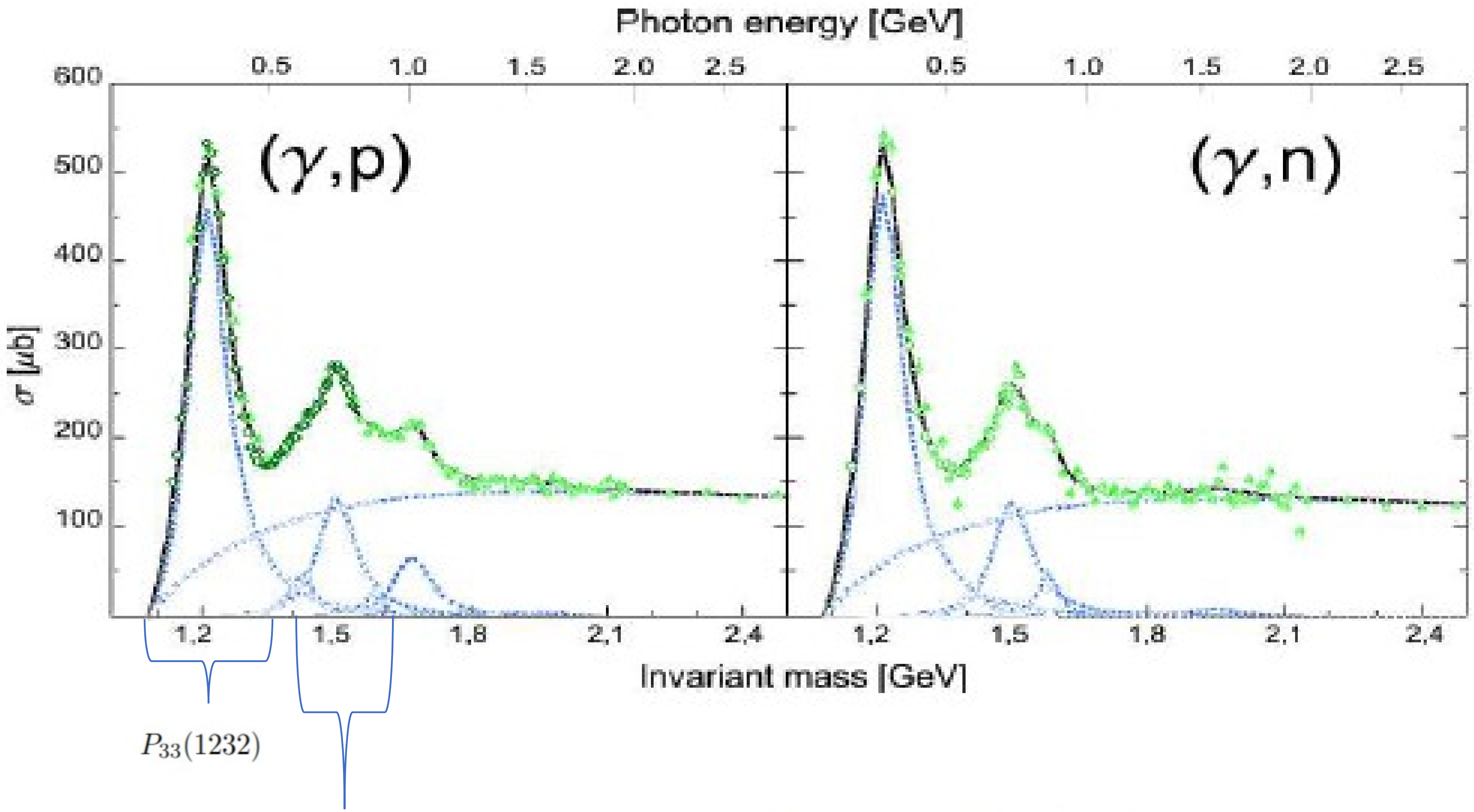

Second resonant region: $P_{11}(1440), D_{13}(1500), S_{11}(1535)$

Motivations of the research

Partial Wave Analysis on differential cross section and polarization observables

S-type experiment: $\frac{d\sigma}{d\Omega}$,Σ,T,R

$$\frac{d\sigma}{d\Omega} = \frac{1}{2}\frac{q^*}{k^*}\left(H_1(\theta)^2 + H_2(\theta)^2 + H_3(\theta)^2 + H_4(\theta)^2\right)$$

$$\Sigma = \frac{q^*}{k^*} Re(H_4^* H_1 - H_3^* H_2) / \frac{d\sigma}{d\Omega}$$

$$R = -\frac{q^*}{k^*} Im((H_3^* H_1 + H_4^* H_2)) / \frac{d\sigma}{d\Omega}$$

$$T = \frac{q^*}{k^*} Im((H_2^* H_1 + H_4^* H_3)) / \frac{d\sigma}{d\Omega}$$

Scalar meson photoproduction

- 8 possibile combination of helicity states
- 4 indipendent matrix elements for the transition operator.
- 16 observables for these amplitudes

too many!

Vector meson photoproduction

The number of observables increases.

GRAAL facility

- Higly polarized beam of γ ray photons.
- **Possibility to access to Beam Asimmetry measurements Σ.**
- **Polarizzation observables impose more constraints to model parameters than angular cross section.**

Motivations of the research

Analysis of the channel $\gamma p \rightarrow \eta' p$ and data CLAS

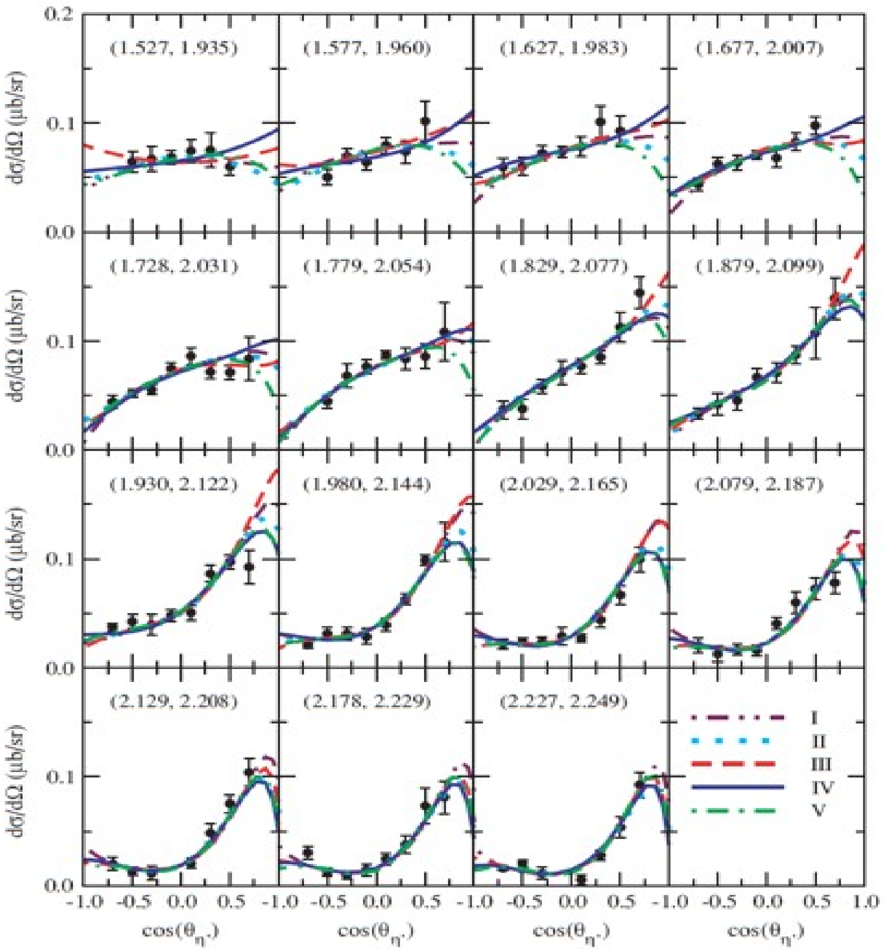

Differential cross section measurements compared with 5 different ipothesis of a model

K. Nakayama, H. Haberzettl, Phys. Rev. C 73, 045211 (2006).

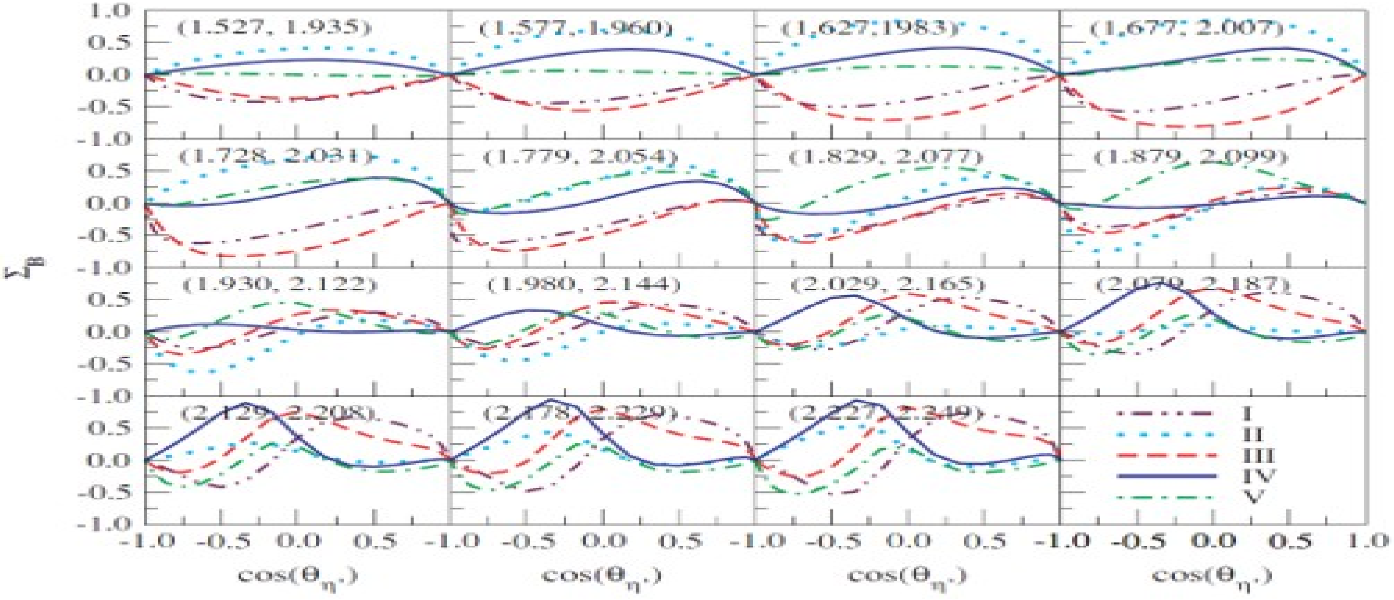

Calculated values of Beam Asymmetry polarizzation with the same ipothesis , compared with CLAS data.

Very different behaviour!

Beam Polarization Asymmetry measures are complementary to differential cross section ones

Motivations of research: analysis of the $\gamma p \to \eta' p$ channel.

New recent beam asymmetry measurements form BGOeggs.

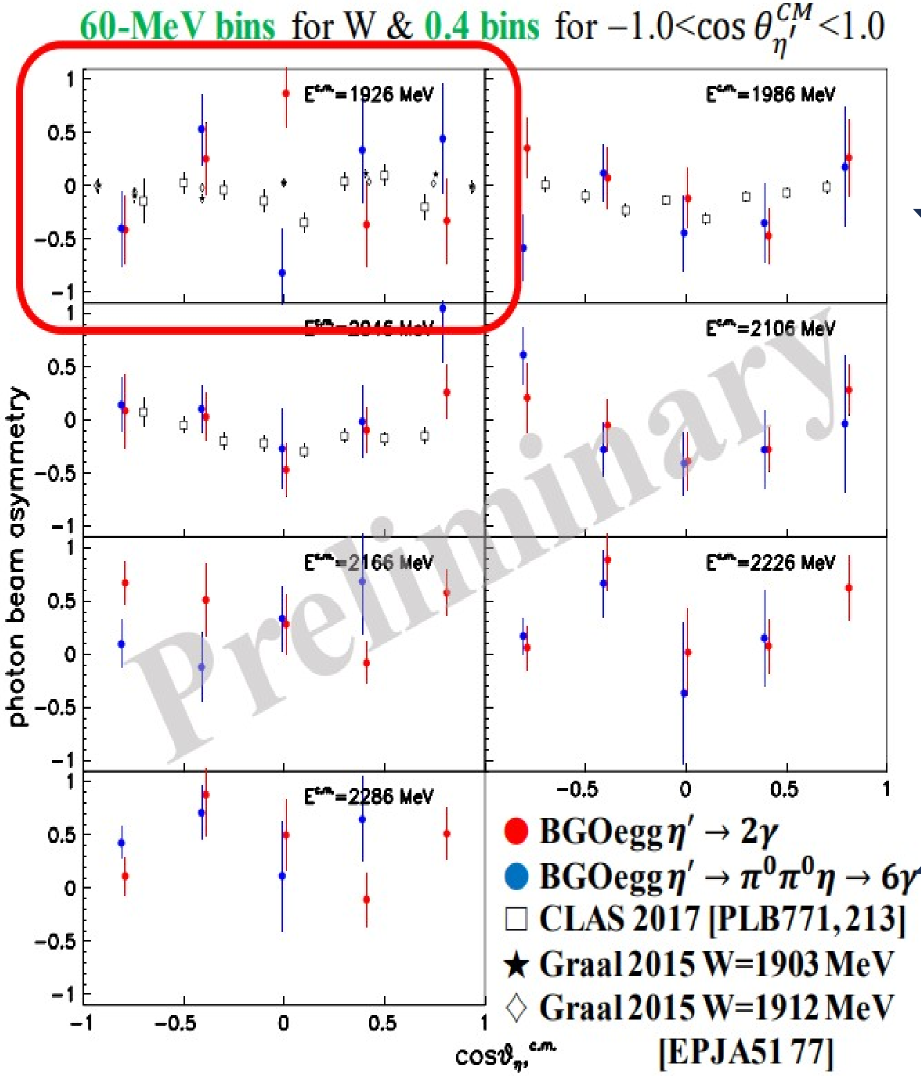

Measurements of LEPS experiment,presented by Tohoku University at Hadron2023

L. Tiator,1, * M. Gorchtein,1, Eta and Etaprime Photoproduction on the Nucleon with the Isobar Model EtaMAID2018

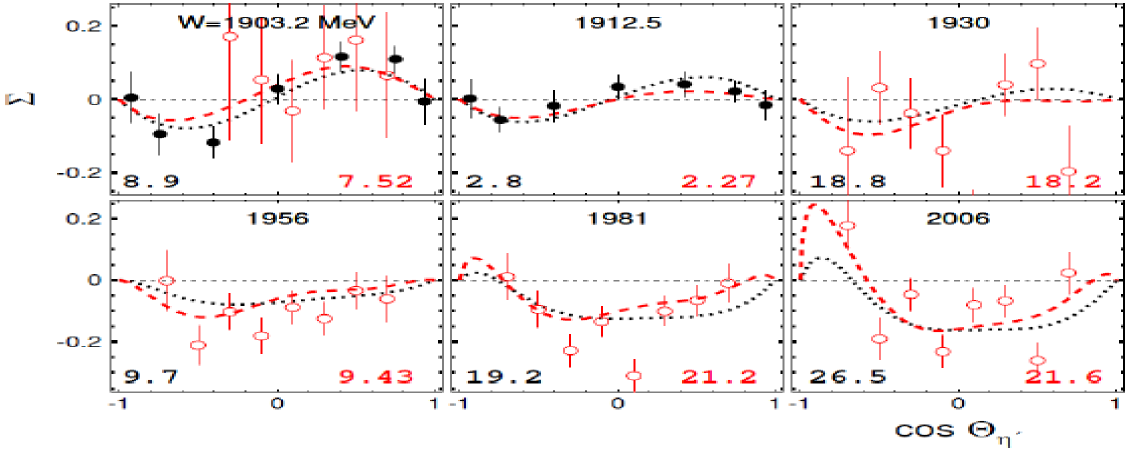

L. Tiator ETAMAID: S11(1900) resonance, **Bonn-Gacthina**: D13(1900) resonance.

A.V. Anisovich a,b , V. Burkert c, Proton-η' interactions at threshold

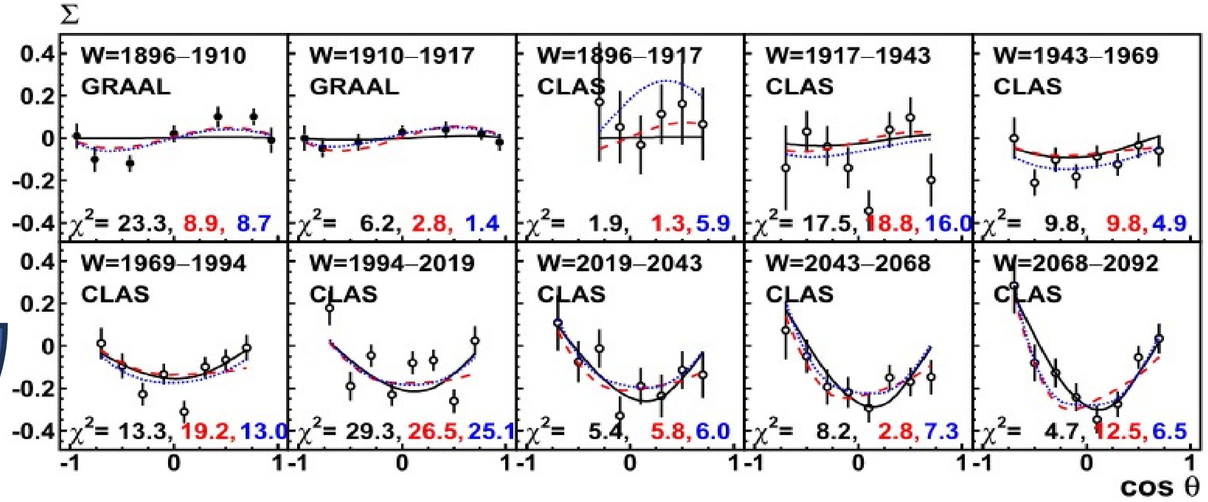

Black line: fit assuming no resonance, **blue curve: fit assuming a resonance** , **red curve: fitting assuming a resonance j=.** .

Description of the apparatus

GRAAL(Grenoble Anneaux Radiation Acceleratour Laser)
Esperiment conducted at accelerator facility ESRF(Grenoble) France

Apparatus

- Polarized gamma rays beam production
- Hydrogen or deuterium liquid target
- Detection system Layrange 4
- Tagging System.

Trigger System

- Acquisition of physical events
- Acquisition of beam events

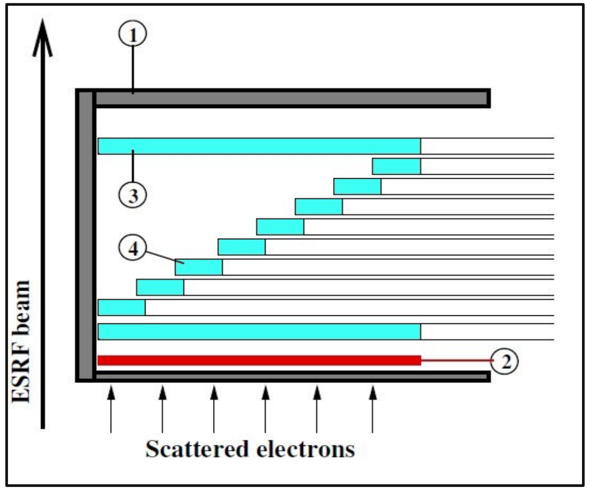

Tagging system
1) 128 Cu strip.
2) Two long plastic scintillators.
3) 8 short plastic scintillators.

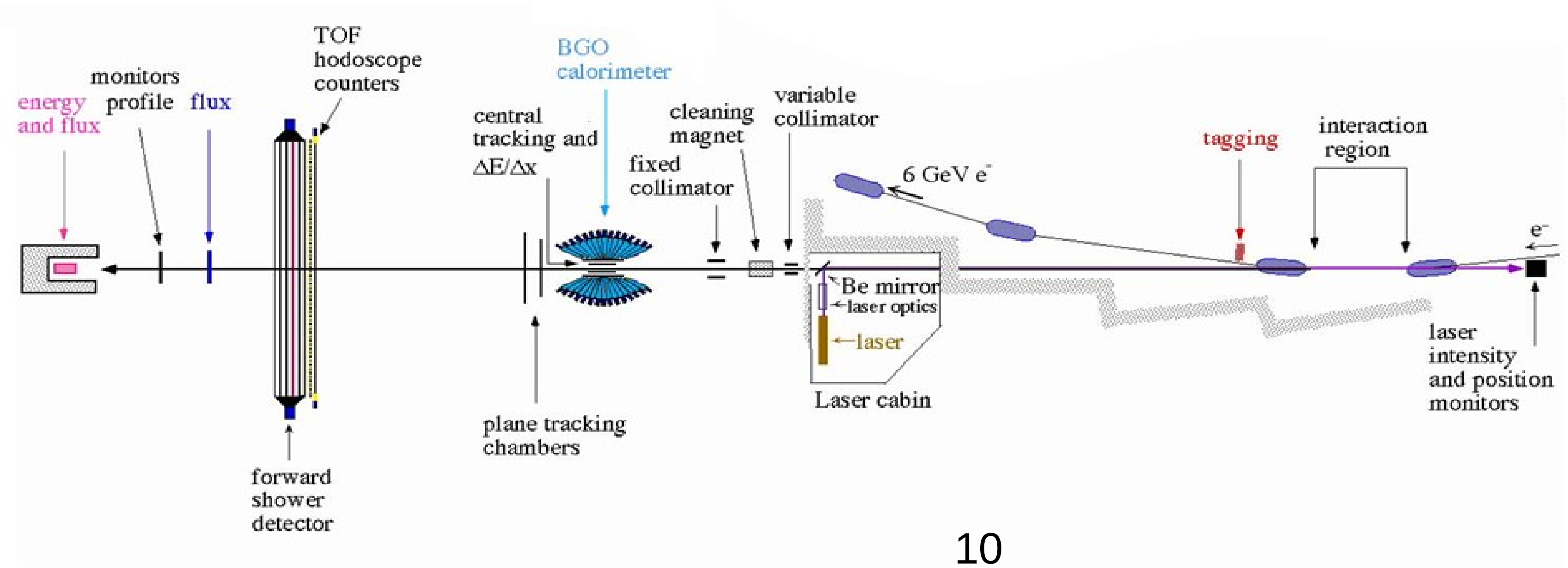

Description of the apparatus: backscattering Compton

Gamma rays beam production
Backscattering Compton of laser photons against ultrarelativistic electrons of the storage ring of the ESRF.

Kinematics of Backscattering Compton

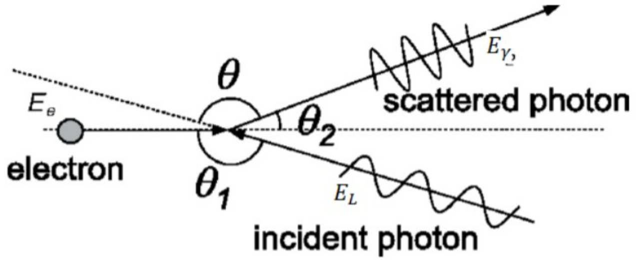

$$E_\gamma = \frac{4\gamma^2 E_L}{1 + \frac{4\gamma E_L}{m_e} + \theta^2\gamma^2}$$

Tagging System
Energy of gamma photons was determined by measuring distance of scattered electrons from electron beam in the storage ring of ESRF.

Helicity of ultrarelativistic electron is conserved in the scattering with laser photon

Maximum transfer of polarization degrees of freedom from photons laser to gamma photons

Access to Polarization Beam Asymmetry measurements

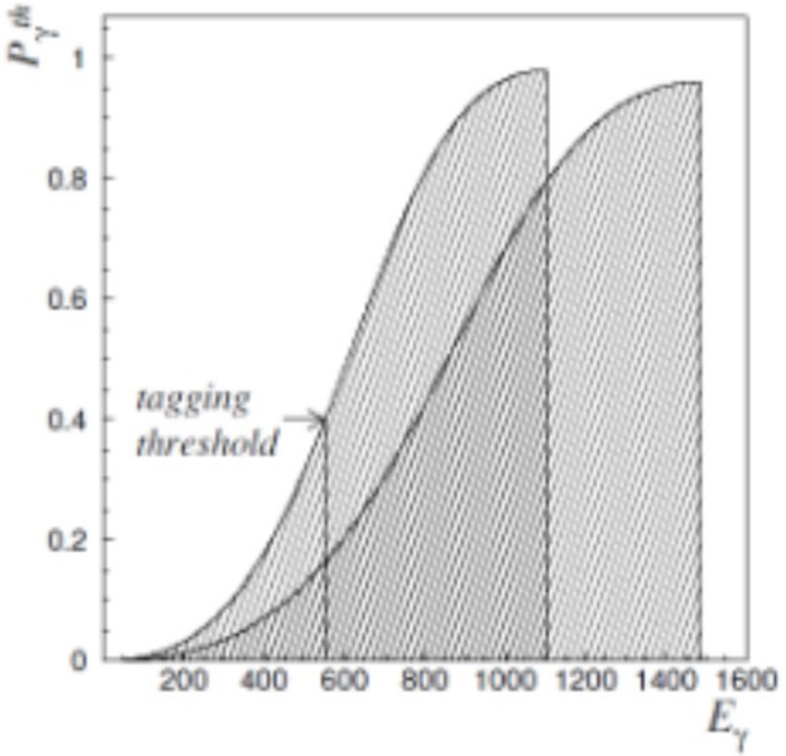

Polarization very close to 1 at energy threshold for the reactions $\gamma N \to \eta' N$

Description of the apparatus

Thin monitor structure
3 plastic scintillators with an aluminum sheet placed between the first and the second plastic scintillator.

Efficiency of the thin monitor measured by the contemporaneous presence of the thin monitor and the spaghetti monitor (eff. ~100%).

Triggers for the acquisition of the beam events

- Coincidence of the last two plastic scintillators + anti-coincidence with the first one.
- Coincidence between a signal in the thin monitor and a signal in the tagging system.

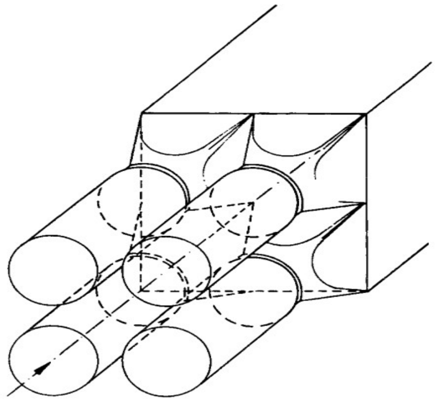

View of spaghetti monitor

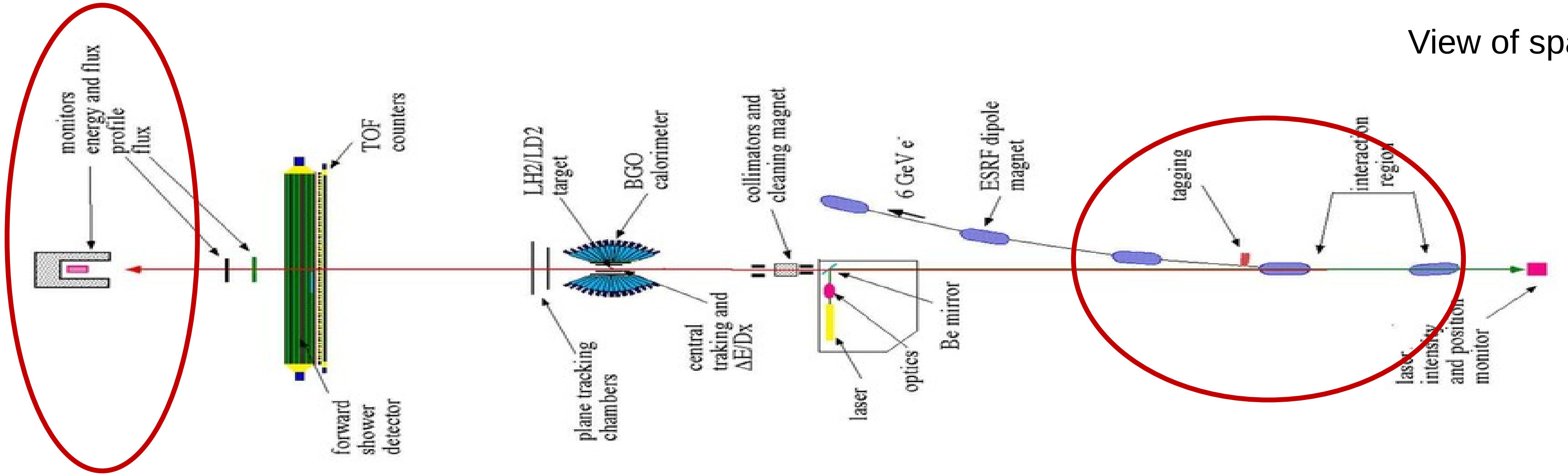

Description of the apparatus: Layrange Detection System: Central section

2 cilindrical Multiwire proportional chambers (MWPC)
1 Used for tracking central charged particles.
2 Angular resolutions: 1.5 % θ , 1.9 % Φ.
Stripped cathodes with anodic wires, emedded in a gas mixture 80 % Argon, 20 % ethanol.

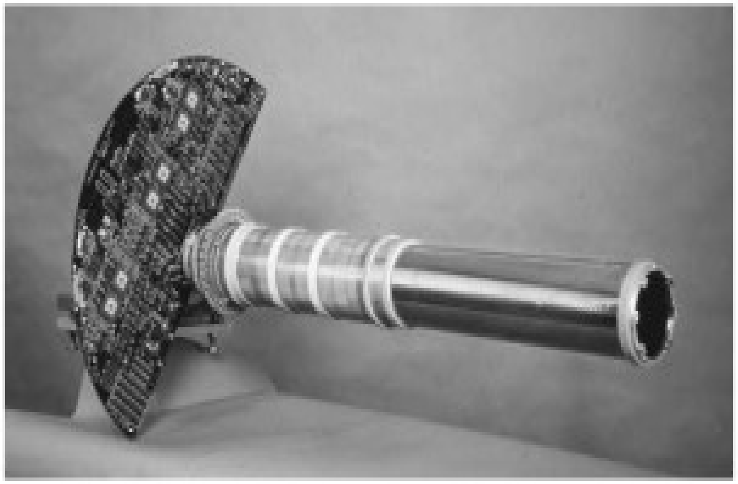

Barrel of plastic scintillators
DE/dx measurements of charged particles.

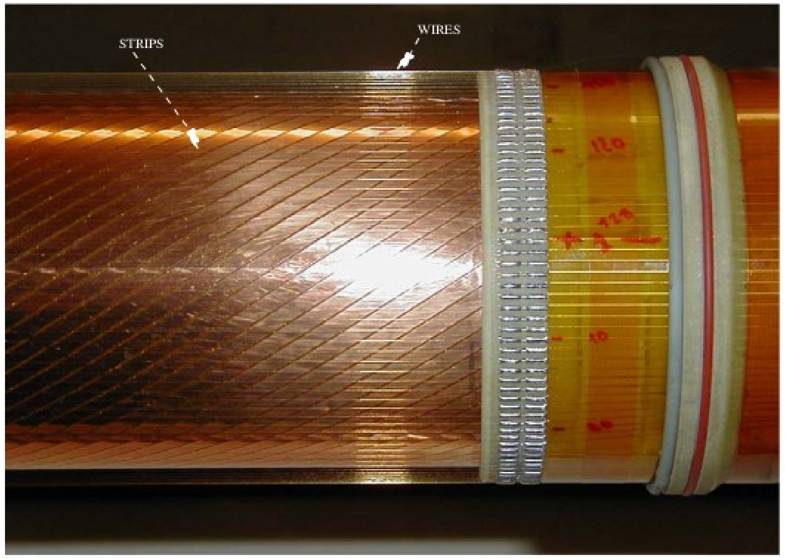

BGO calorimeter
- Measurement of the energy and angles for central photons.
- Energy measurements for central charged particles(residual energy of protons).

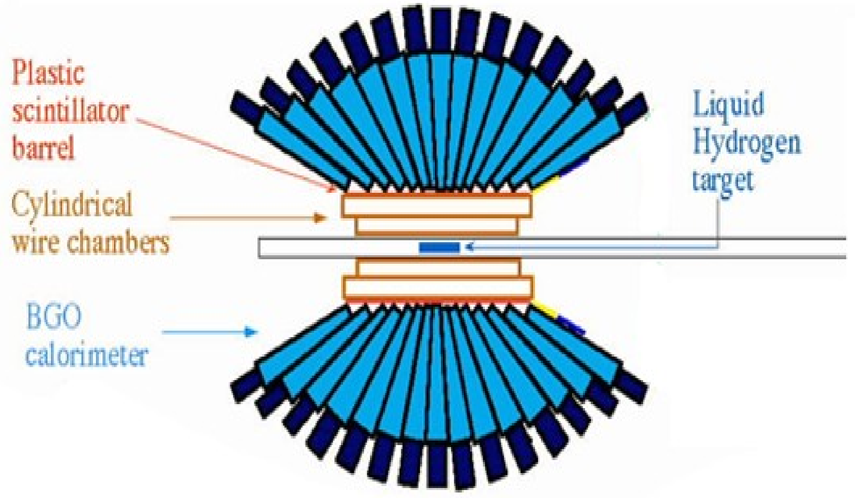

BGO Calorimeter
- 450 crystals of Bismute Germanate(BGO) arranged in this way:
- 15 crystals covering the polar plane.
- 32 crystals covering the azimuthal plane.

Discrimination between charged and neutral particles
Neutral track: only hit in the BGO.
Charged tracks: hits in MWPC chambers- barrel- BGO

Description of the apparatus: forward section of Layrange detection system

Two planar MWPC
measures of angles of charged particles.

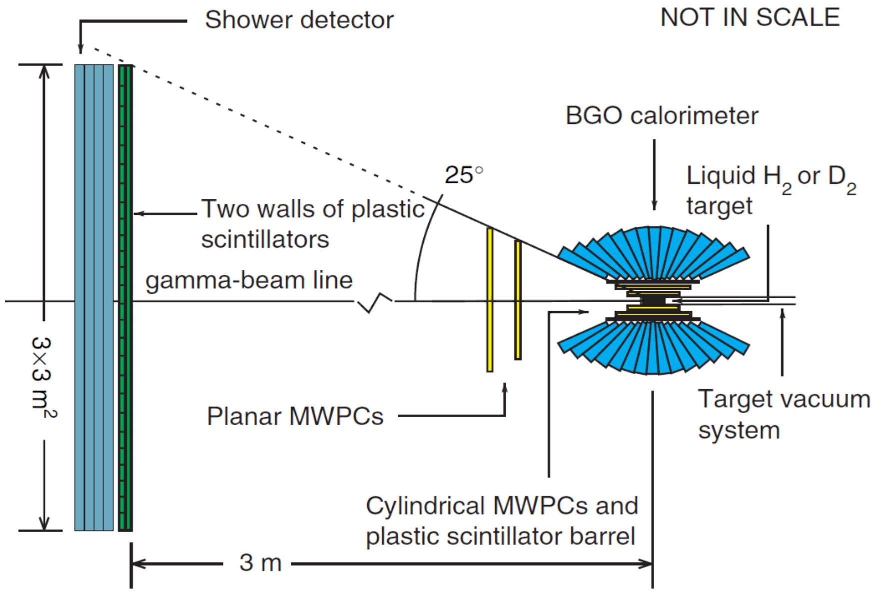

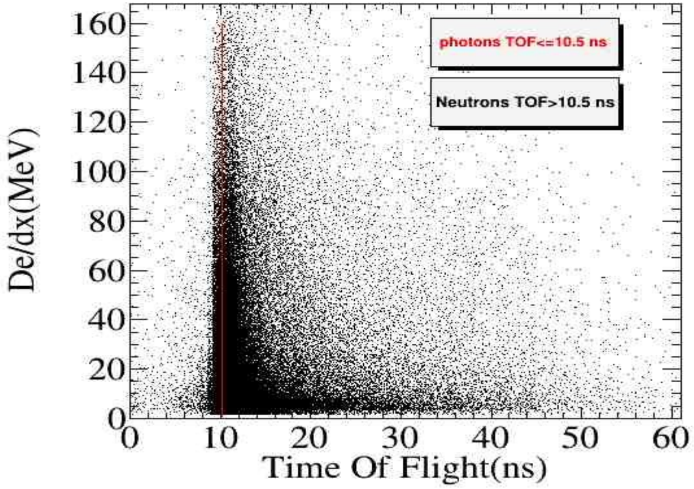

Double plastic-scintillator Shower wall

- Identification of charged and neutral particles.
- Measure of angles of both charged and neutral particles.

Identification of charged and neutral particles with the T.O.F vs dE/dx tecnique

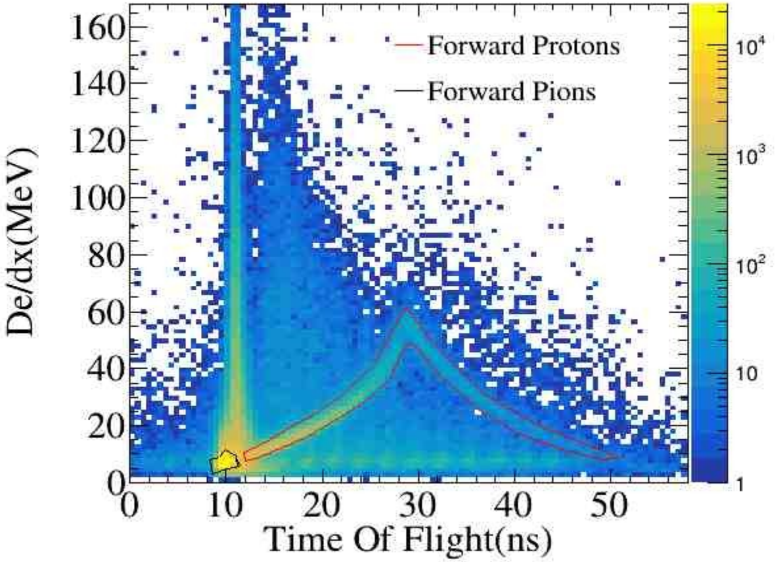

Hodoscope

- Identification of charged particles.
- Measure of angles of cahrged particles

Analysis and results

Events selection by imposing kinematical cuts on the Neutron missing mass distribution:

$$M_n^{mis} = \sqrt{(E_\gamma + M_n - E_n)^2 - (P_\gamma - P_n^z)^2 - (P_n^y)^2 - (P_n^x)^2}$$

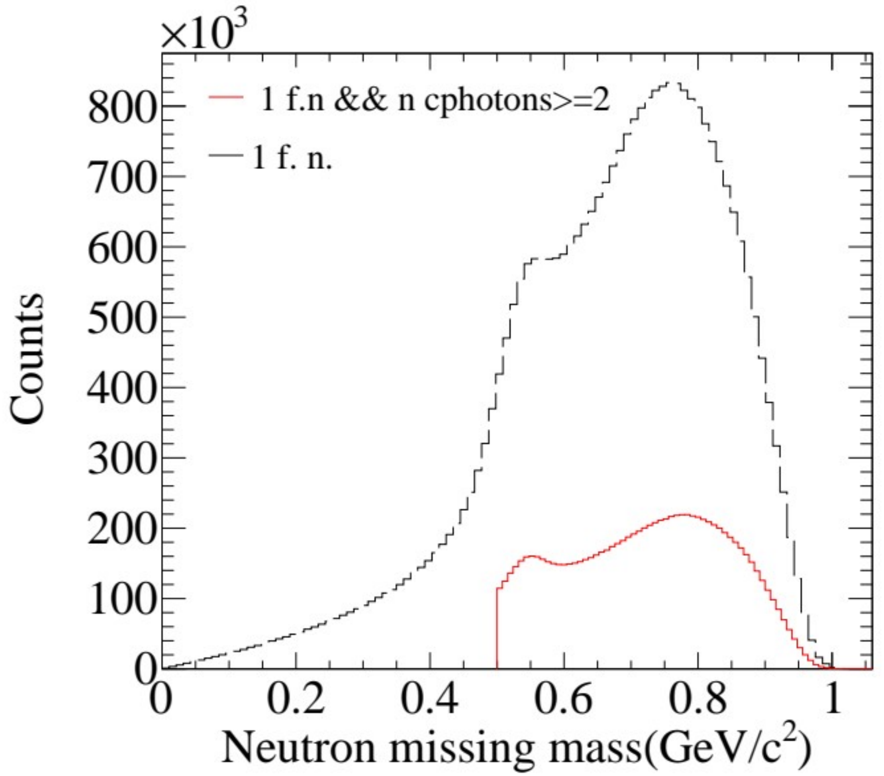

Analysis and results

Events selection by imposing kinematical cuts on the Neutron missing mass distribution:

$$M_n^{mis} = \sqrt{(E_\gamma + M_n - E_n)^2 - (P_\gamma - P_n^z)^2 - (P_n^y)^2 - (P_n^x)^2}$$

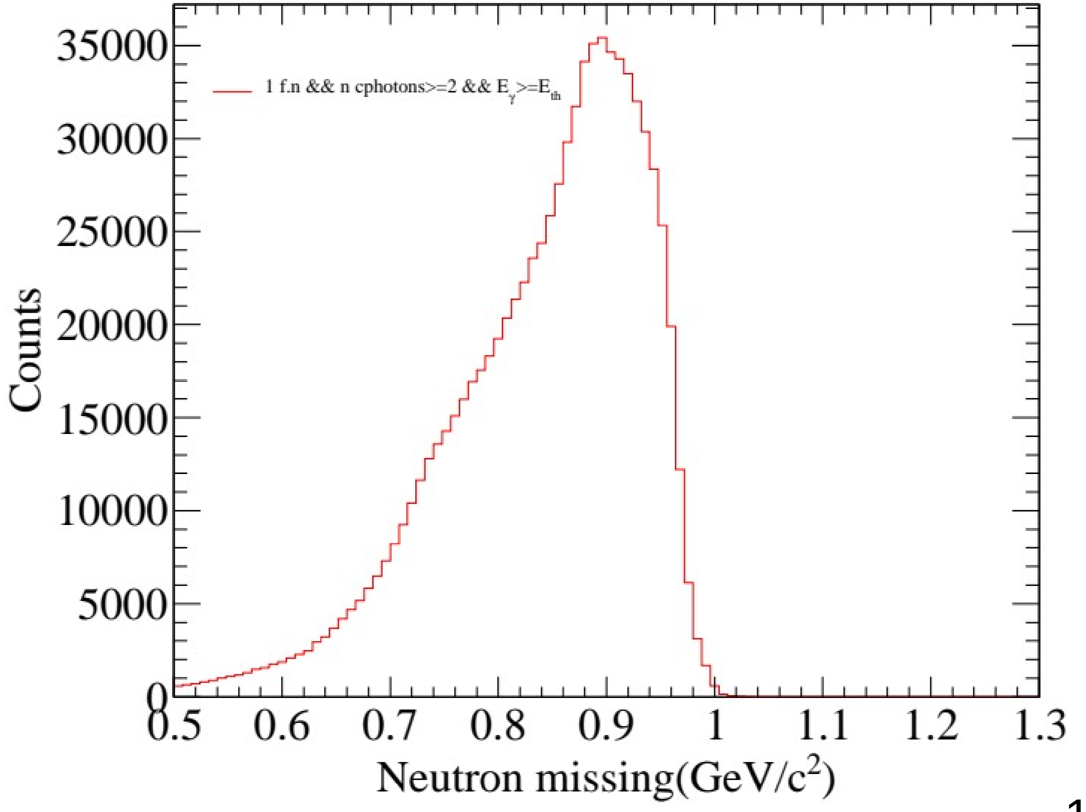

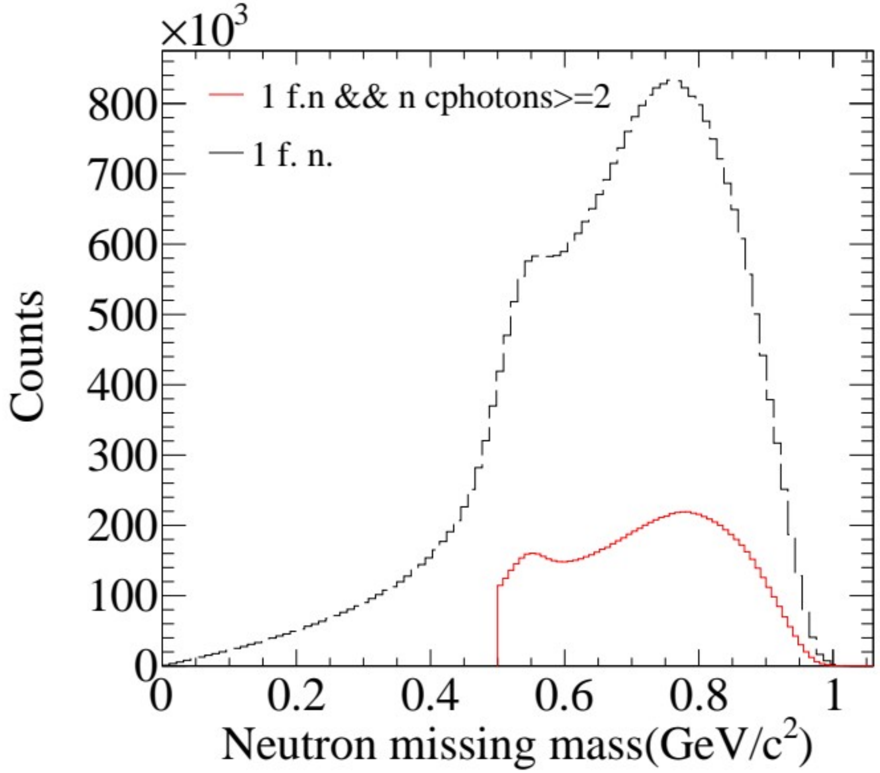

η' ??

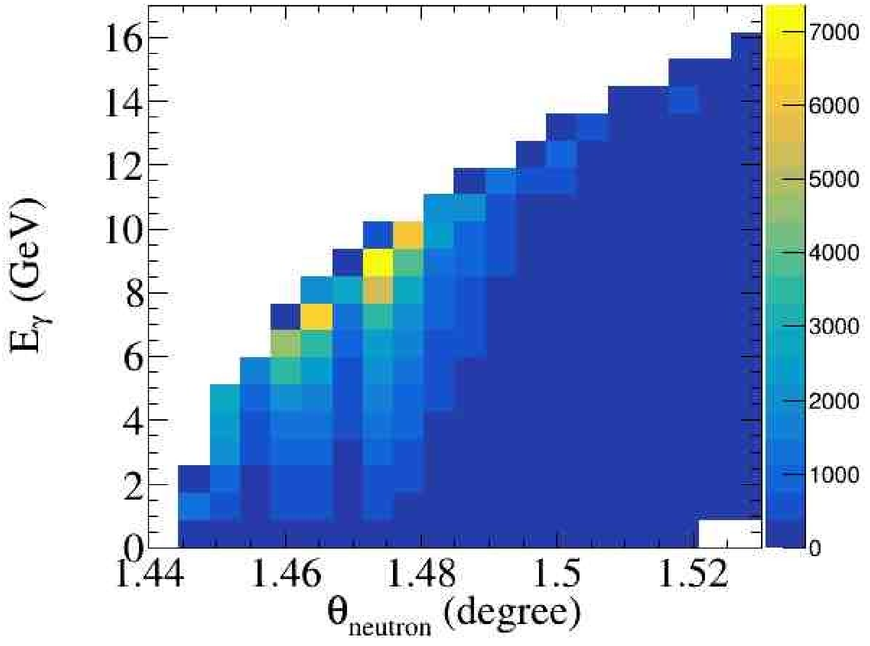

Simulated distribution Eg vs θ_n

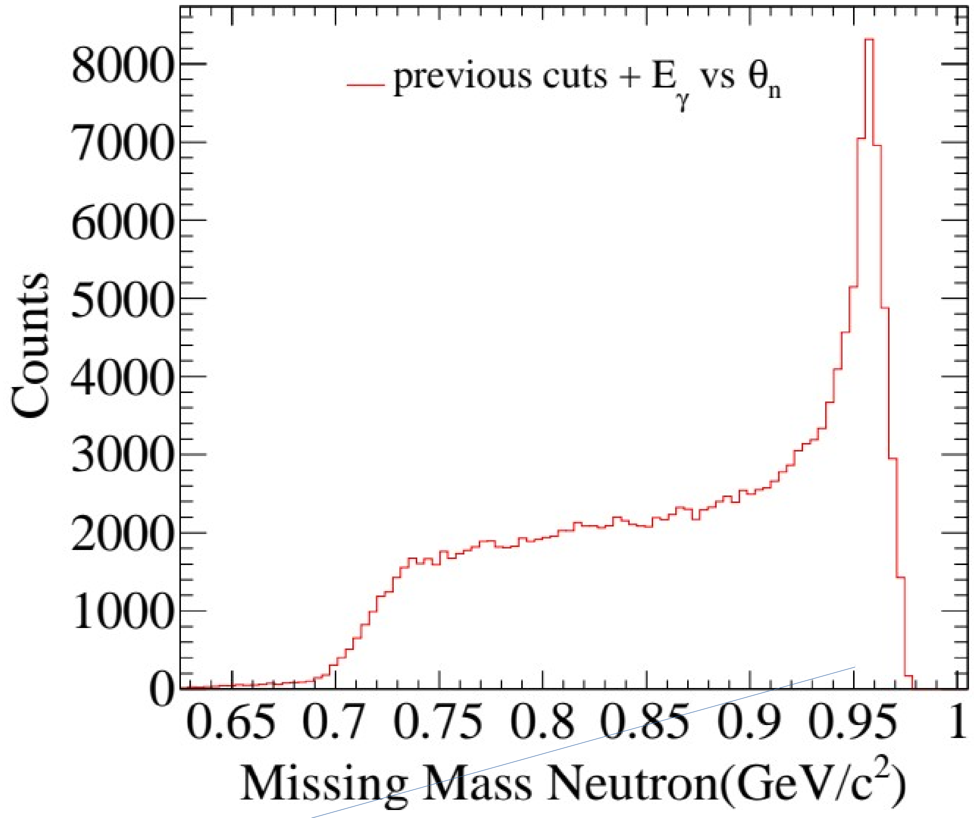

$$M_{n'} = 0.95778\ GeV/c^2$$

Applying a selection on the four momentum components of the neutron.

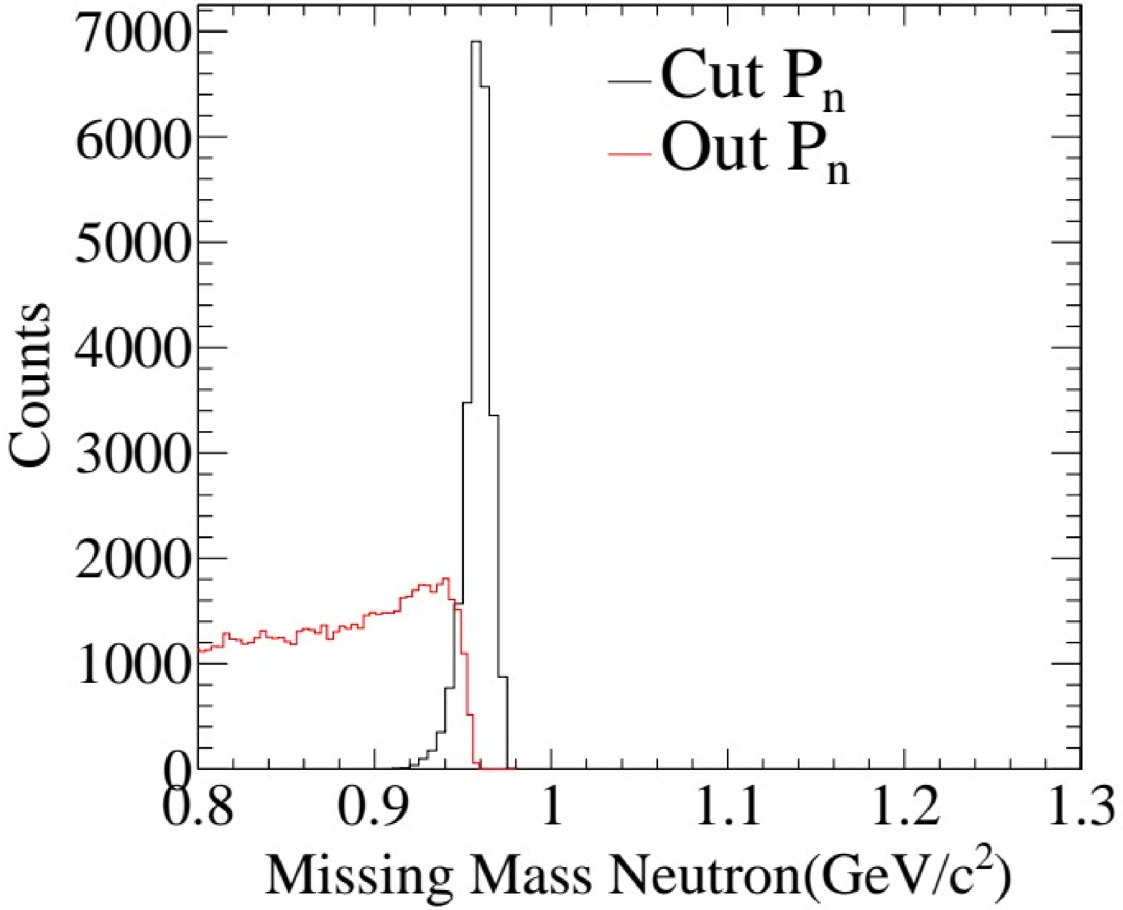

Analysis and result

Subsequently to remove the residual background, we applied other cuts:

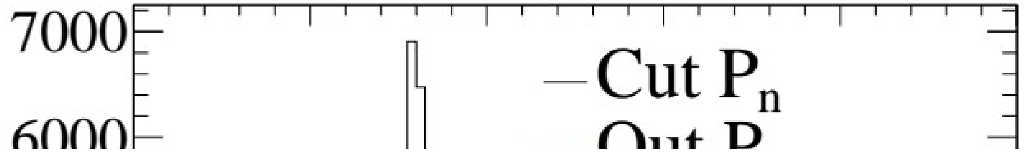

Applying a selection on the four momentum components of the neutron.

A cut Energy of γ photon vs energy of neutron based on a simulation.

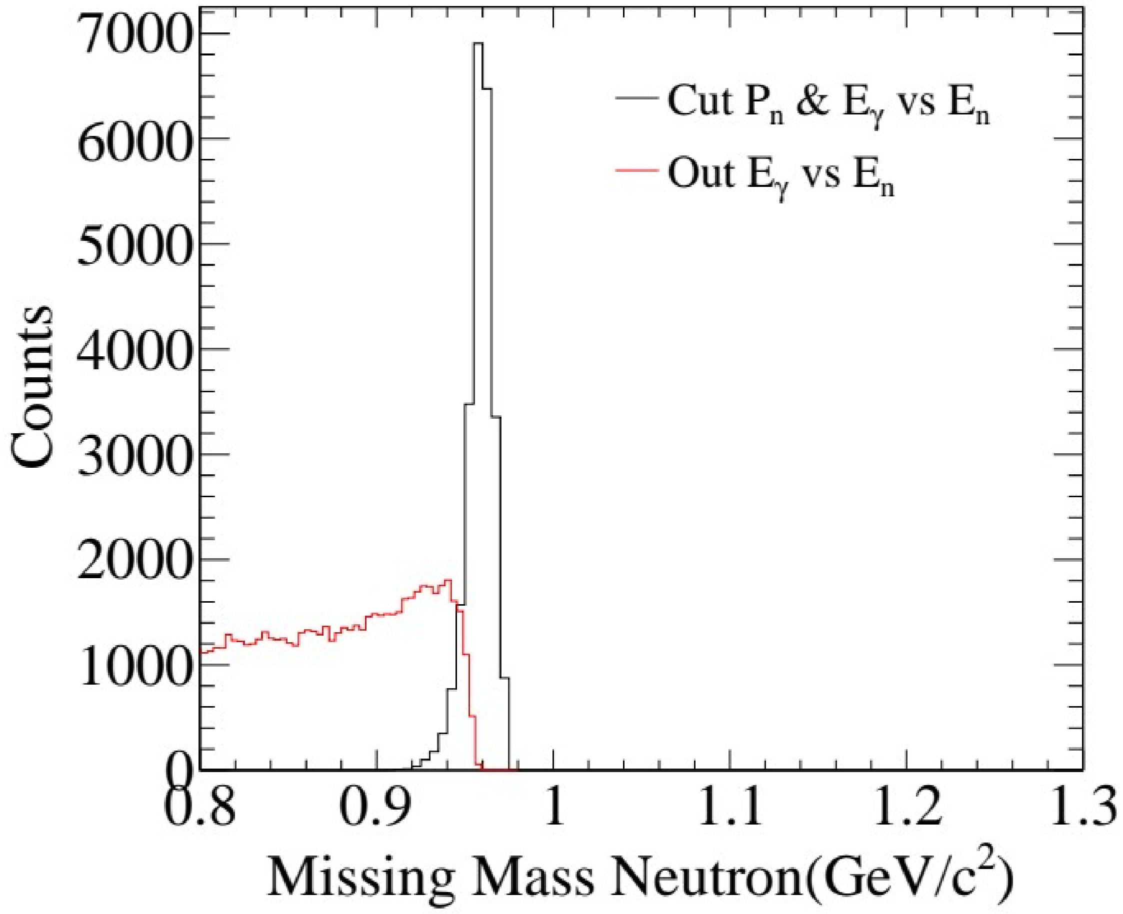

Analysis and results

Beam Asymmetry Σ measurements for η' photoproduction on neutron bound in deuterium

Beam Asimmetry measurements
<Eg> = 1.461 GeV,
Five intervals in : [0°,25°], [25°,45°], [75°,105°], [120,145],[145,180]

The Beam Asimmetry Σ is extracted from the fit of the following ratio:

$$\frac{\frac{N_V}{F_V}}{\frac{N_V}{F_V}+\frac{N_H}{F_H}} = \frac{1}{2}(1 + P_\gamma \Sigma cos(2\phi))$$

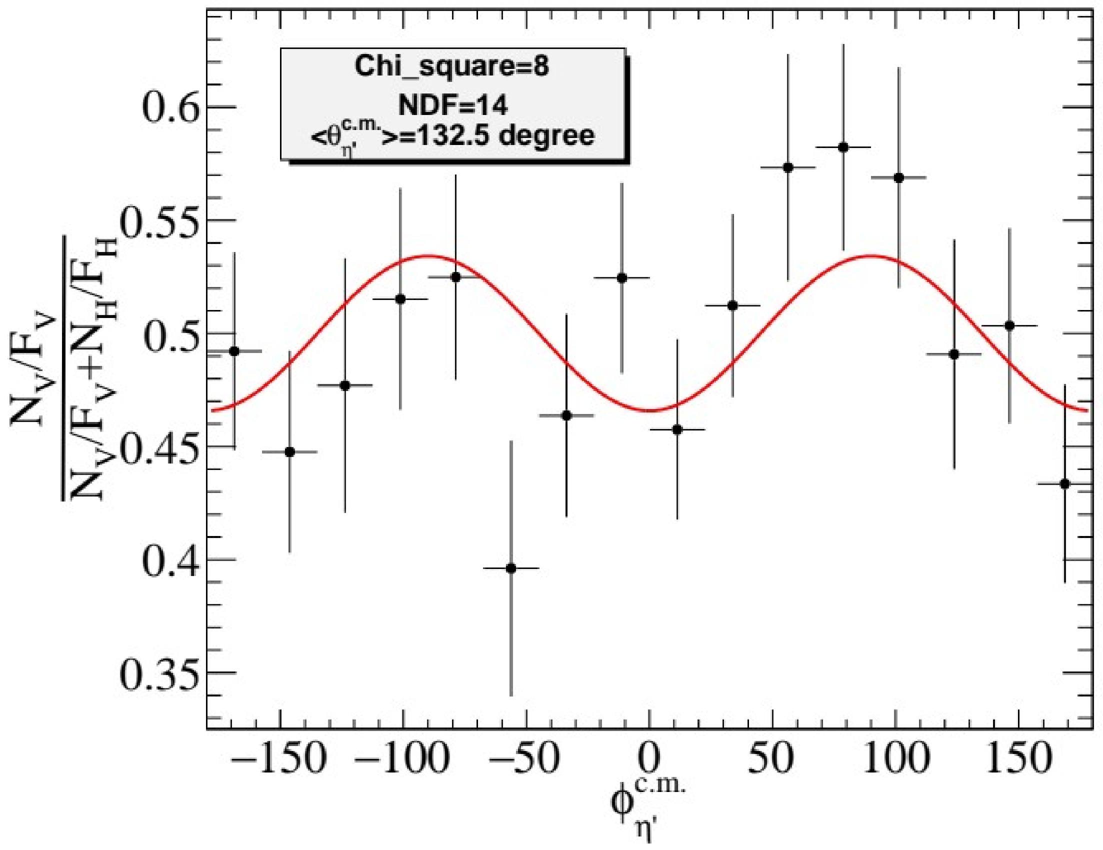

Analysis and results

Comparison between our preliminary Beam Asimmetries measurements for the neutron channel with the Beam Asymmetries measurements for the proton channel.

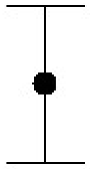

Beam asymmetry measurements of the GRAAL collaboration for the channel $\gamma p \rightarrow \eta' p$

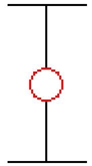

Our beam asymmetry measurements for the channel. $\gamma n \rightarrow \eta' n$

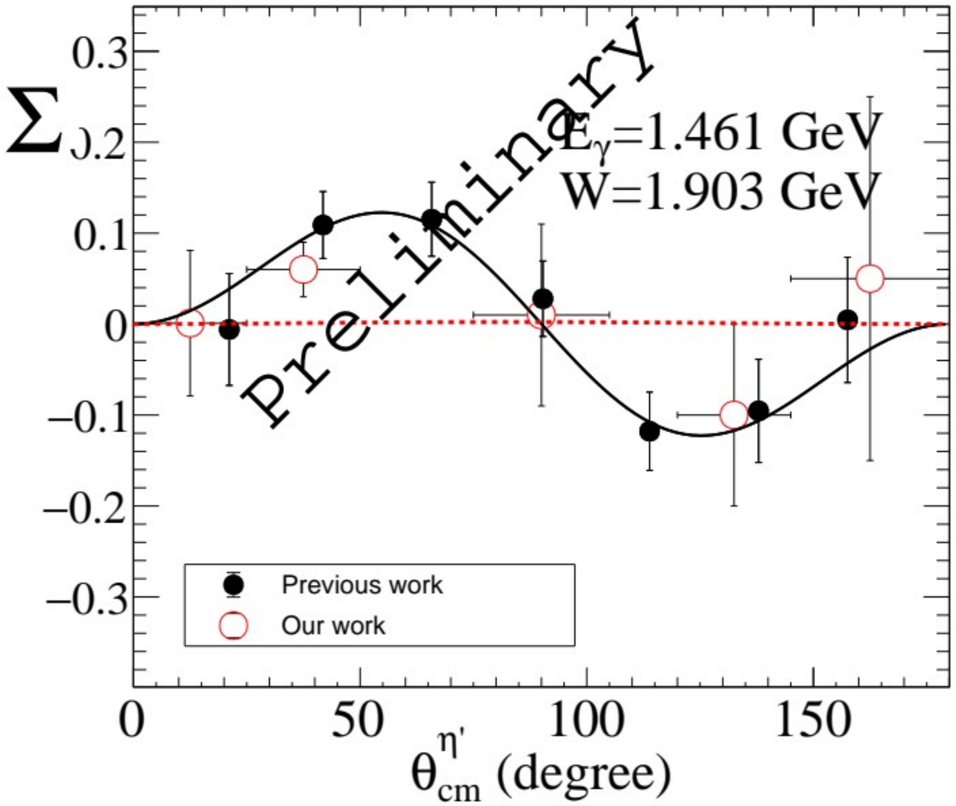

Conclusions

1) We have extracted the first estimations of the Beam asimmetry measurements for the η' photoproduction channel on neutron.

2) We have compared our measurements with the ones for the η' photoproduction channel on proton, confirming the structure observed for the proton channel.

3) We will accomplish new analysis on this data, first of all the substraction of the residual background.

What else to do?

- Investigation of the current channel by a simulation(in progress).
- Investigation of the η' photoproduction channel on bound protons inside deuterium atoms(in progress).

Thank you all for your attention !

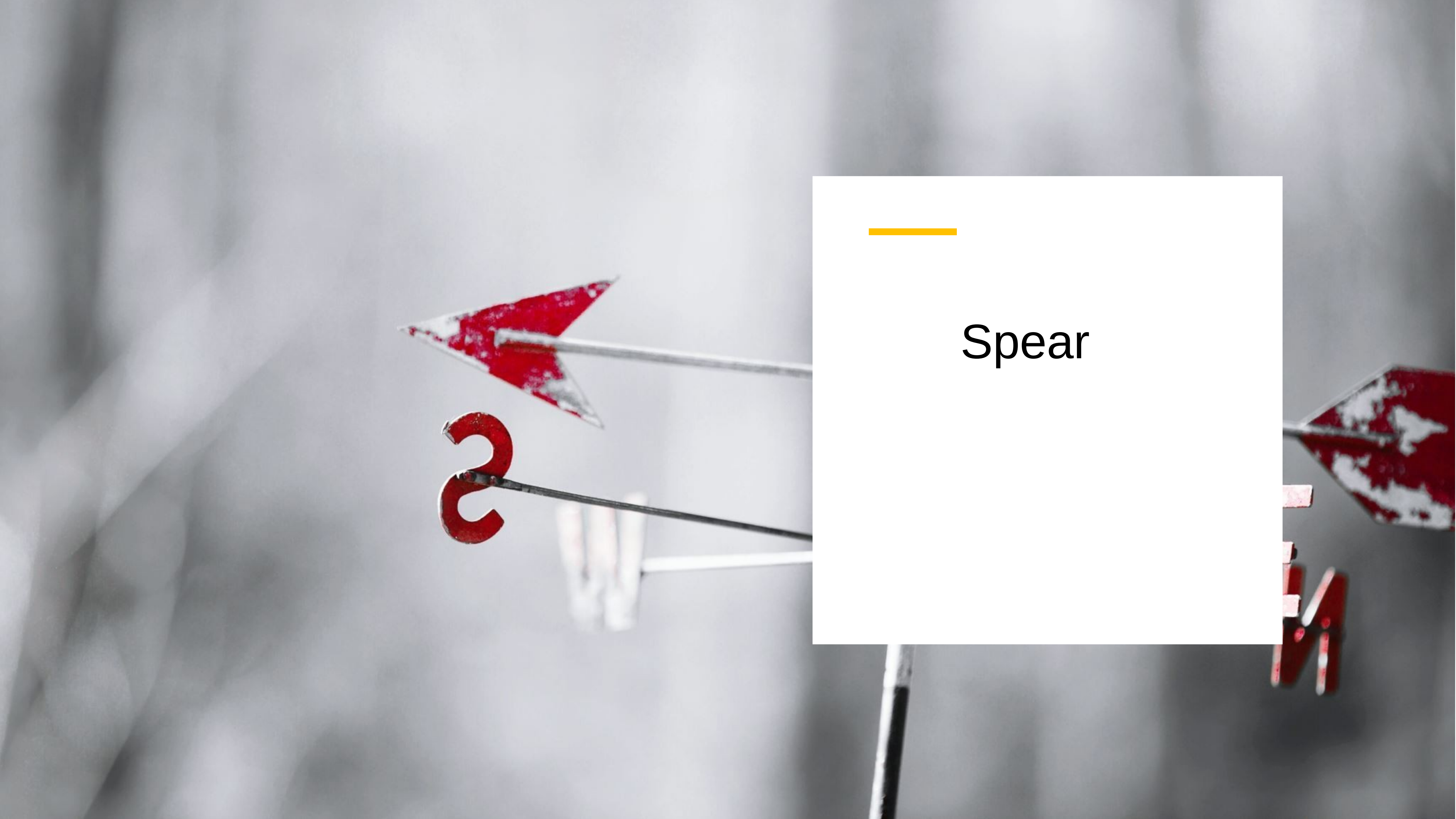

Spear

Isospin transition amplitude consists of a vector part A^V3 isoscalar term A^IS, isovector term A^IV

$$A^{IS} = \langle \frac{1}{2}, \pm\frac{1}{2} | \hat{S} | \frac{1}{2}, \pm\frac{1}{2} \rangle \qquad \mp A^{IV} = \langle \frac{1}{2}, \pm\frac{1}{2} | \hat{V} | \frac{1}{2}, \pm\frac{1}{2} \rangle \qquad A^{V3} = \langle \frac{3}{2}, \pm\frac{1}{2} | \hat{V} | \frac{1}{2}, \pm\frac{1}{2} \rangle \, .$$

$$\begin{aligned}
A(\gamma p \to \pi^+ n) &= -\sqrt{\frac{1}{3}}\, A^{V3} + \sqrt{\frac{2}{3}}(A^{IV} - A^{IS}) \\
A(\gamma p \to \pi^o p) &= +\sqrt{\frac{2}{3}}\, A^{V3} + \sqrt{\frac{1}{3}}(A^{IV} - A^{IS}) \\
A(\gamma n \to \pi^- p) &= +\sqrt{\frac{1}{3}}\, A^{V3} - \sqrt{\frac{2}{3}}(A^{IV} + A^{IS}) \\
A(\gamma n \to \pi^o n) &= +\sqrt{\frac{2}{3}}\, A^{V3} + \sqrt{\frac{1}{3}}(A^{IV} + A^{IS}) \, .
\end{aligned}$$

A(γ +n η′ n) = $A^{IV} + A^{IS}$

A(γ + p η′ p) = $A^{IV} - A^{IS}$

Theoretical works

- **Black line:** function fit**.**
- **Red dotted line:** reggeized model**.**
- **Blue dashed line:** effective Lagrangian approach**.**
- **Green dot-dashed: t**he isobaric model.
- Orange long-dashed: a chiral quark

model approach.

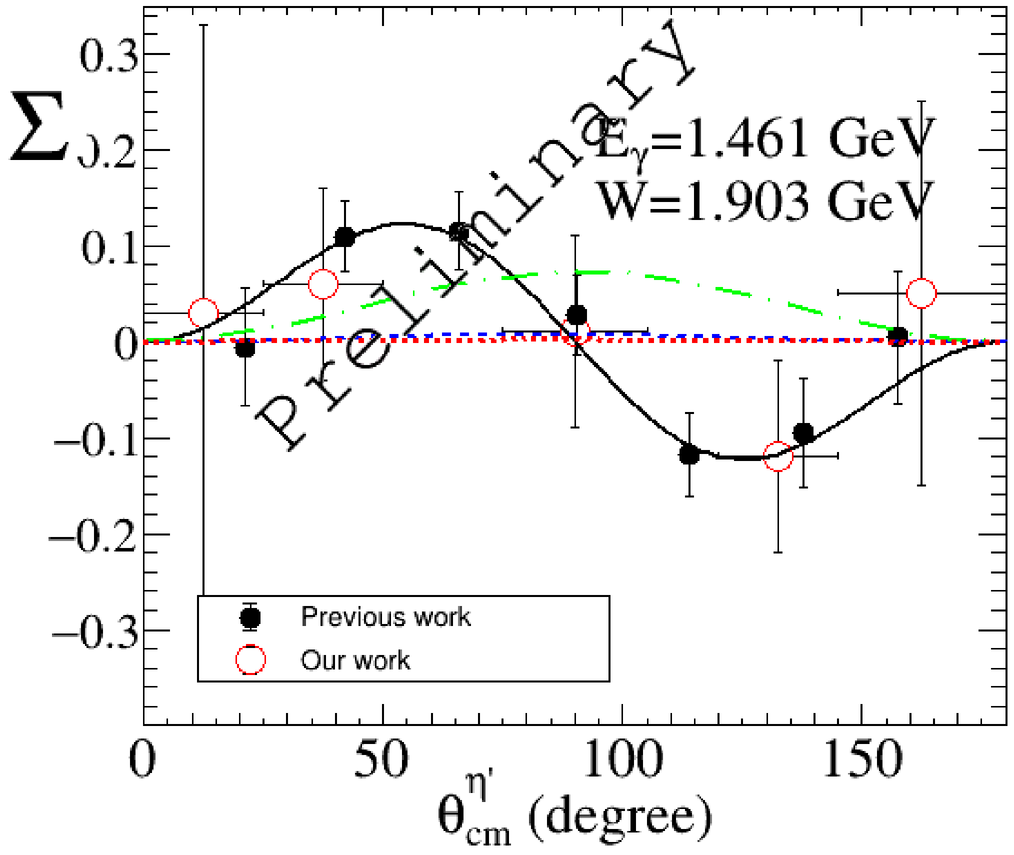

Time of flights measurements of the thin monitor

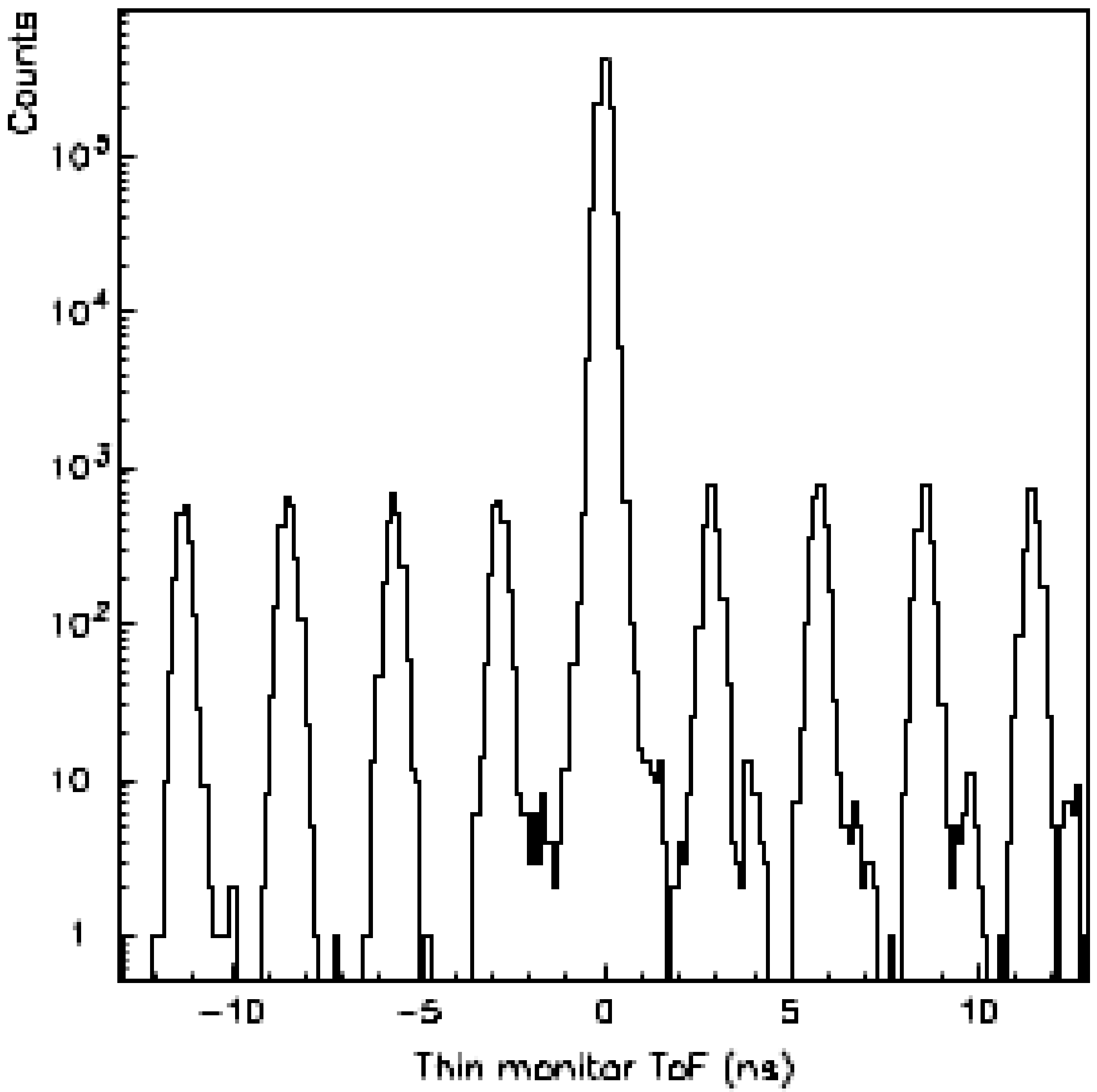

Description of the apparatus :BGO calorimeter

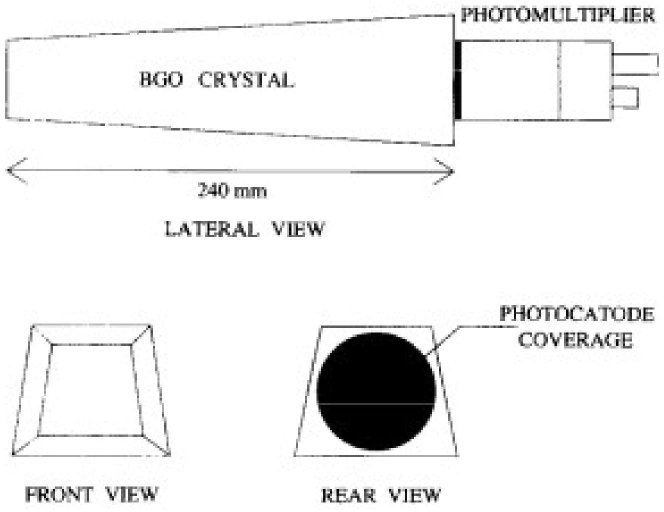

Fig. 3. Schematic views of a BGO crystal.

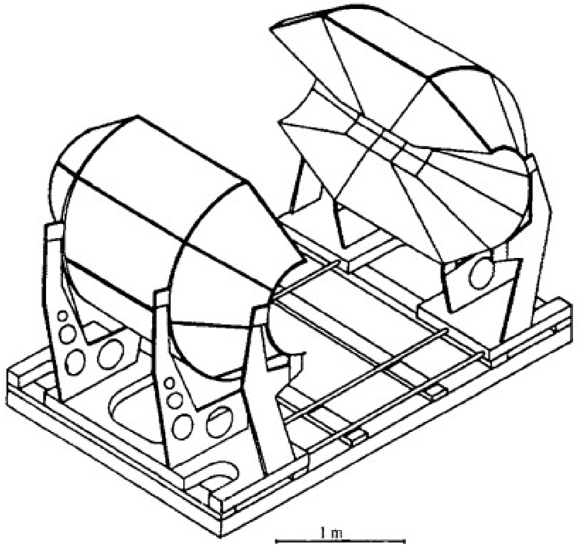

Efficiency for gamma photons and neutrons ~ 100 %, good energy resolutions for low-energy protons.

High energy resolution for gamma photons.

$$\Gamma(FWHM) = \sqrt{a^2 + \left(\frac{b}{E_\gamma}\right)^2 + \left(\frac{c}{\sqrt{E_\gamma}}\right)^2} \simeq 2\%$$

Resolutions of the angles for gamma photons:

$$F_\theta = 6\%, F_\phi = 7\%$$

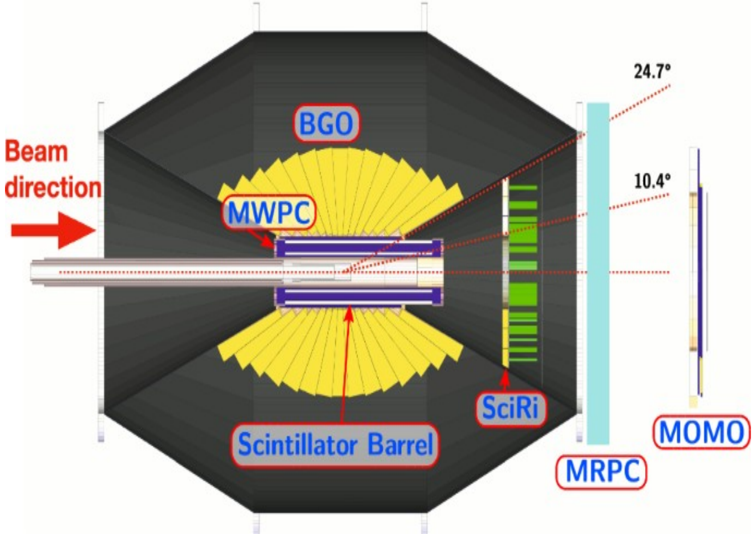

Identifications of charged particles By DE_dx vs Er tecnique, combining loss energy measurements in the bar rel with the energy deposition in the BGO calorimeter.

Acquisiton of physical events
An energy deposition in the BGO calorimeter higher than 300 MeV in coincidence with the tagging system.